Journal of Metallurgical and Materials Engineering, Vol.27, No.2, 2016.

Microstructural Evolution during Friction Stir Welding of Austenitic Stainless Steel AISI 316 to Low Carbon Steel St37

A.H. Khosrovani nezhad[1], M. Shamanian[2],
A. Rezaeian[3], M. Atapour [4]

1- Introduction

Dissimilar joining of austenitic stainless steels and low carbon steels are extensively utilized in many applications. Numerous investigations have been performed to evaluate these dissimilar joints using various methods such as gas-tungsten arc welding, resistance spot welding, friction welding, laser welding and electron beam welding. The common finding of the above researches show that there is a large thermal stress due to the difference in expansion coefficient and thermal conductivity of the dissimilar metals. Furthermore, formation of δ-ferrite, sigma phase and grain boundary corrosion at the joining boundary, as well as separation of alloying elements during solidification have been observed. In order to solve these problems, much research on solid state welding methods has recently been carried out. Friction stir welding (FSW) is one of the relatively new types of solid state welding that has been applied to establish dissimilar butt or lap joints of soft to soft or soft to hard metal. The aim of the present study is to evaluate the microstructure of dissimilar joining between austenitic stainless steel AISI 316 and low carbon steel St37 using FSW.

2- Experimental procedure

The base metals used in the present investigation were plates of AISI 316 austenitic stainless steel and St37 steel. Table 1 shows the nominal chemical composition of the as-received steels.

Table.1 The chemical composition of the base metals (wt.%)

St 37	0.09	0.01	0.02	0.01	Bal.
AISI 316	0.05	16.3	11.7	2.59	Bal.

The used plate were 100 mm long, 60 mm wide and 1.5 mm thick and a butt joint design was selected for welding. The FSW tool, made of WC-based material, had a shoulder diameter of 16 mm, truncated cone pin with tip pin diameter of 3.5 mm and end pin diameter of 4.5 mm and 1.25 mm pin length. A vertical milling machine was employed for the welding experiments and FSW was conducted using a rotational speed of 600 rpm and welding speed of 50 mm/min. In the present work the St37 steel was placed on the retreating side (RS) and the 316 steel on the advancing side (AS) of the weld. Argon shielding gas was blown around the tool at a flow rate of 18 L/min in order to prevent the surface oxidation. The stir zone temperature was measured by a K-type thermocouple placed at the bottom surface of the plates. The maximum measured temperature was about 950 °C. Microstructural studies were carried out using an optical microscope (OM) and a scanning electron microscope (SEM) equipped with an energy-dispersive X-ray spectroscopy (EDS) analysis system. The carbon steel was etched using 2% nital solution and the stainless steel was electrolytically etched using a 60% HNO_3 solution at 5-10 V for 5-10 s.

3- Results and discussion

To study the possible formation of carbides and intermetallic compounds during the welding process, XRD analysis was carried out as shown in Fig. 1. It seems that in spite of the rising temperature during welding, no other phases except the ferrite and austenite phases are present.

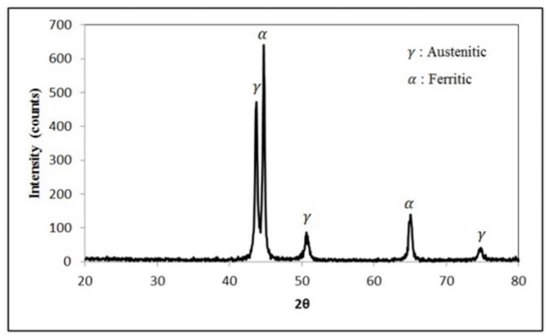

Fig.1 XRD pattern from the weld sample

In order to examine the interface boundary more accurately, spot and line scan analysis using EDS were carried out, as shown in Fig. 2. As depicted in this figure, elemental Fe, Cr, Ni and Mo were found to be distributed across the interface. It is also observed that by moving from the St37 steel towards the 316 steel side, the amounts of Cr, Ni and Mo solute atoms increased while the amount of Fe decreased.

Fig. 3 shows a low magnification image of the cross section of the welded sample. As can be seen, it contains several microstructural regions. Besides the base metals (regions 1 and 6) other microstructural regions can be identified as follows:

Region 2: Heat affected zone (HAZ) on the St37 side
Region 3: Stir zone (SZ) on the St37 side
Region 4: Stir zone (SZ) on the 316 side
Region 5: Thermo-mechanically affected zone (TMAZ) on the 316 side

---

[1] * Corresponding Author, M.Sc. Student, Department of Materials Engineering, Isfahan University of Technology.
[2] Professor, Department of Materials Engineering, Isfahan University of Technology.
[3] Assistant Professor, Department of Materials Engineering, Isfahan University of Technology.
[4] Assistant Professor, Department of Materials Engineering, Isfahan University of Technology.

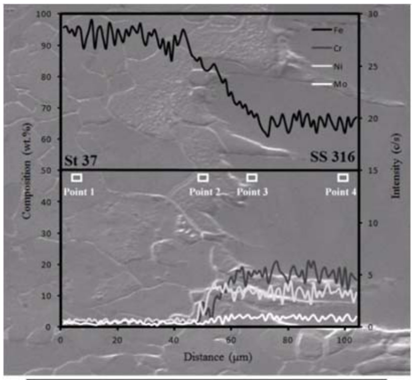

wt.%				
	Point 1	Point 2	Point 3	Point 4
Fe	92.9	83.1	66.3	64.1
Cr	2.4	8.4	16.8	18.5
Ni	2.8	6.8	13.2	13.3
Mo	1.9	1.8	3.5	4.7

Fig. 2 EDS spot and line scans across the boundary of the two steels in the SZ

Fig. 3 Different microstructural regions in the cross-section of the welded sample

The TMAZ region is a narrow area between the base metal and the SZ region in the 316 steel (as indicated in Fig. 3). Fig. 4 shows the microstructure of the TMAZ showing the deformed austenite grains. The material in the TMAZ region experiences lower temperatures and strains as compared to the SZ region.

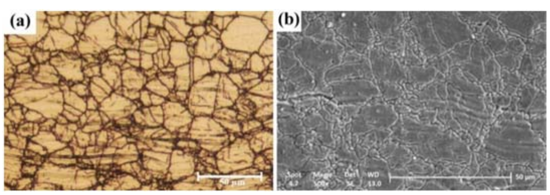

Fig. 4 (a) OM and (b) SEM micrographs of the TMAZ in 316
Steel

Fig. 5 shows the SZ region in the welded sample on the St37 steel side. The temperature in this region is higher than the A3 temperature therefore, the ferritic–pearlitic microstructure in this region has transformed to austenitic during the process. The average grain size in this region is 9.1 µm.

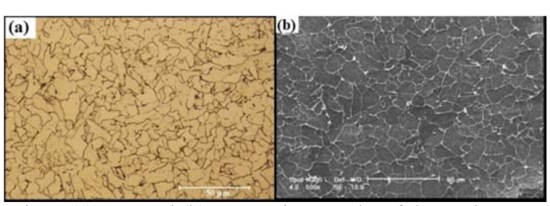

Fig. 5 (a) OM and (b) SEM micrographs of the SZ in St37 steel

Fig. 6 shows the SZ region in the welded sample on the 316 steel side. As can be seen, in contrast to the St37 steel, DDRX has occurred in this region, mainly because there was no phase transformation during cooling. Therefore, comparing the SZ regions in the two steels (Fig. 5 and 6), it can be seen that grain refinement has occurred in the stainless steel, whereas it did not take place on the St37 side. The average grain size in this region is 4.9 µm.

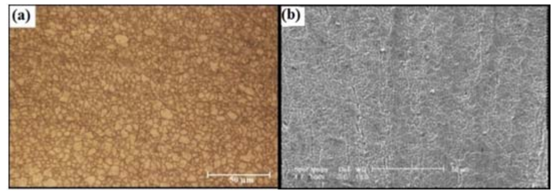

Fig. 6 (a) OM and (b) SEM micrographs of the SZ in the 316 steel

4- Conclusions

The results of phase investigations showed that in spite of the diffusion of alloying elements, no carbides and brittle phases were detected at the joining boundary. Microstructural investigations showed that the highest decrease in grain size occurred in the stir zone region on the austenitic stainless steel side.